

Finite Element Analysis of Paddler Sludge Dryer for its Structural Integrity under Different Loading Conditions

Manoj A. Kumbhalkar ^{1*}, Tukaram S. Sargar ², Suhas H. Sarje ³, Manish Sakhlecha ⁴,
Sunil Prayagi ⁵, Gaurav Gondhlekhar ⁶, Nitin B. Kardekar ¹, Mrinal Sorte ¹

¹ Department of Mechanical Engineering, JSPM Narhe Technical Campus, Pune, India

² Department of Mechanical Engineering, Smt. Kashibai Navale College of Engineering, Pune, India

³ Department of Mechanical Engineering, Jayawatrao Sawant College of Engineering, Pune, India

⁴ Department of Civil Engineering, Raipur Institute of technology, Raipur, India

⁵ Department of Mechanical Engineering, Yeshwantrao Chavan College of Engineering, Nagpur, India.

⁶ Department of Electrical Engineering, Yeshwantrao Chavan College of Engineering, Nagpur, India.

*Corresponding author E-mail: manoj.kumbhalkar@rediffmail.com

Received: April 3, 2025, Accepted: July 3, 2025, Published: July 18, 2025

Abstract

The paddler sludge dryer machine made on standard parts & mechanisms are made from special grade material i.e. SS316, SS304 & MS Etc. To ensure functional accuracy and robust structure of sludge drying machine which is subjected to different load conditions thus The Finite Element method was (FEA) used to study structural integrity of design of the paddle sludge dryer under different load conditions the assembly of paddle sludge dryer is studied using finite element analysis (FEA) under different loads like structural and thermal loads. Modal analysis of assembly is done to analyze the natural frequency of structure to verify it for the resonance condition. The induced stresses in assembly due to structural and thermal loads are within the allowable limits of stress while the assembly natural frequencies of vibration are far from the motor excitation frequency thus the resonance condition is not likely to happen during motor running operation. Based on FE analysis results, paddle sludge dryer assembly is safe under the provided operating conditions.

Keywords: Modal analysis, Thermal analysis, Structural analysis, FEA, Boundary conditions.

1. Introduction

This paper addresses the Finite Element Analysis (FEA) of Paddle Sludge Dryer in assessing its structural integrity under different loading conditions. The work is carried out in the company that specializes in the production of woodworking equipment and machinery. The objective of the project is to analyse the performance of the dryer with a focus on ensuring structural stability and efficiency under different loads using ANSYS software. The paddle sludge dryer, an essential part of Technogem's product portfolio, has been engineered to help remove moisture from sludge-a semi-solid by-product of numerous industrial processes-so that it becomes less environmentally hazardous and easier to handle.

The overall treatment of the sludge entails processes such as thickening, dewatering, and drying. Thickening is carried out with the assistance of gravity thickeners that lower the water content. Next, dewatering decreases the moisture content further so that the sludge can be processed as a solid. The drying phase employs thermal drying, which treats the substance by evaporation of water. Due to their efficiency and lower environmental damage, indirect drying methods are preferred, including the use of steam or thermal oil as heat carriers.

Dry sludge has multiple applications, including agricultural use, soil conditioning, construction activities, and landfill covers. Paddle sludge dryers are widely utilized for functions like drying, heating, cooling, pasteurization, and crystallization. The dryers are known to be effective against high temperatures, structural loads, and vibrations.

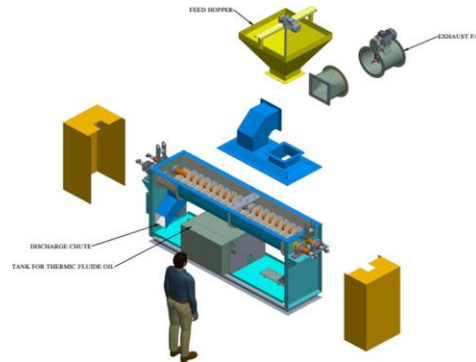
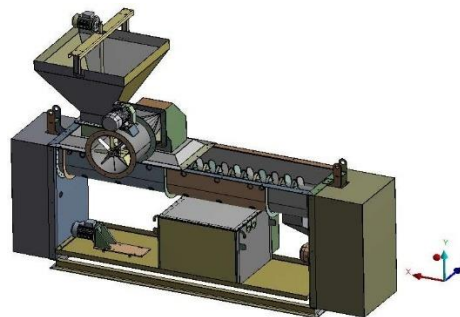
The principal objective of the project is to study the structural integrity of the paddle sludge dryer under heat, structural, and vibration loads through FEA. The analysis will confirm whether the dryer assembly is safe at operating conditions or design optimization should be carried out. The project scope includes structural, thermal, and modal analysis, which ensures the performance, longevity, and safety of the design under varying conditions.

The geometry and the CAD model of the paddle sludge dryer was created and imported into ANSYS19 R3 to carry out Finite Element Analysis to check its structural integrity under different loading conditions. The material SS 316 is used for the assembly and its properties are as given in table 1.

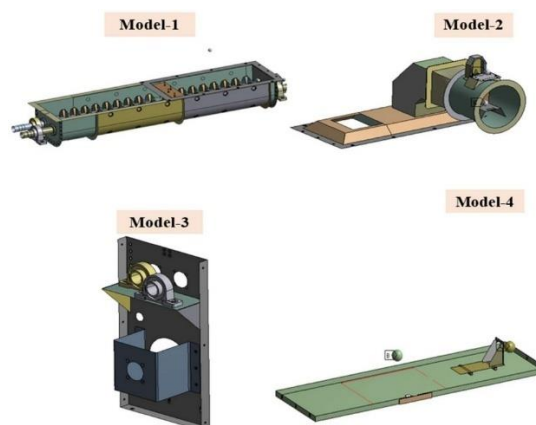
Table 1: Material Properties of SS 316

Property	Value	Unit
Modulus of Elasticity	193000	N/mm ²
Poisson's Ratio	0.30	-
Density	7850	Kg/m ³
Yield Strength	290	N/mm ²
Ultimate Tensile Strength	580	N/mm ²
Thermal Conductivity	60.5	W/m°C

The CAD model of the paddle's sludge dryer is as shown below. Total Weight of the assembly being 1184.5kg.

**Fig 1:** Paddle sludge dryer & its components**Fig 2:** Assembly model of Paddle Sludge Dryer

To carry out the analysis effectively the model is split into 4 parts as shown below:

**Fig 3:** Geometries of four models of paddle sludge dryer

2. Related work

Recent research has also focused on wastewater sludge drying. Bennamoun et al. [1] (2013) reviewed wastewater sludge drying techniques including convective, conductive, and solar drying. Demir [2] (2015) optimized an indirect sewage sludge heat dryer for cost-effective sludge incineration. Chen et al. [3] (2016) compared paddle and disc dryers, finding paddle dryers more effective for sludge viscosity zones. Flori et al. [4] (2020) examined temperature and phase ratios during sludge drying using finite element analysis. Deng et al. [5] (2013) analyzed heat transfer characteristics in indirect paddle dryers. Sapmaz et al. [6] (2016) assessed energy efficiency of paddle dryers for drilling mud drying. Arlabosse et al. [7] (2016) developed a methodology to improve paddle dryer energy design. Wang et al. [8] (2019) created a mathematical model to simulate heat transfer in paddle dryers. Zhang et al. [9] (2016) investigated high-temperature molten salt

flow and heat transfer in paddle dryers. Nimbarte et al. [10] (2015) studied stress analysis of pistons under thermal and pressure loads to enhance performance.

Various studies have investigated thermal and vibrational analysis using Finite Element Analysis (FEA) for mechanical components. Bhagat et al. [11] (2012) analyzed thermal stress distribution in I.C. engine pistons under real engine conditions, highlighting mesh optimization techniques. Havale et al. [12] (2017) applied thermos-mechanical decoupled FEM to study thermal stresses on aluminum alloy piston surfaces using ANSYS. Sau et al. [13] (2022) conducted a comparative study on thermal and dynamic analysis of disc brakes using ANSYS to evaluate different thermal characteristics. Kamalakar et al. [14] (2014) designed a truck oil pan for vibration reduction using FEM, focusing on pre-stress forces and harmonic response analysis. Zhang et al. [15] (2014) analyzed interference fit models in piping systems, identifying abnormal stress distribution through FEA and experimental tests.

In addition, structural dynamics studies comprise Rajappan et al. [16] (2013), who studied truck chassis dynamics when subjected to static loading conditions, and Pandya et al. [17] (2018), who investigated vibration characteristics of pump shafting systems. Equivalent research by Ramu et al. [18] (2012) concentrated on natural frequencies of isotropic thin plates, whereas Pingulkar et al. [19] (2016) worked on cantilever composite plates. Hariharan et al. [20] (2011) and Yamuna et al. [21] (2014) worked on rotor dynamics and beam vibration analysis, respectively. Weis et al. [22] (2017), Nigade et al. [23] (2012), and Chaphalkar et al. [24] (2015) also worked on vibration characteristics of mechanical components through FEA.

In addition, Darapureddy et al. [25] (2013) studied deflections, stiffness, and natural frequencies of turbine base frames with FEA software like HyperMesh and ANSYS. Hebhal et al. [26] (2019) conducted static structural, modal, and harmonic analysis of car rims to analyze stresses and deformation. Gukendran et al. [27] (2022) studied the mechanical performance of different composite materials for wind turbine blades with ANSYS. Narendranath et al. [28] (2012) conducted mechanical and thermal analyses of gas turbine rotor blades, including modal analysis by ANSYS. Naser et al. [29] (2013) designed a pressure vessel for resistance to thermal and pressure loads and verified the design by FEA.

Other researches by Silori et al. [30] (2015) compared stress behavior and fatigue life of traction gears, while Ooi et al. [31] (2013) performed FEM-based modal analysis of portal axle gear train systems. Vanam et al. [32] (2012) compared MATLAB and ANSYS FEA results of isotropic rectangular plates with classical solutions. Raghavedra et al. [33] (2010) studied the structural behavior of laminated composite mono leaf springs to reduce weight. Vegi et al. [34] (2013) studied connecting rods of forged steel and carbon steel with respect to stress, deformation, stiffness, and weight reduction.

Recent studies have also focused on the use of composite materials and structural optimization. Srinivasan et al. [35] (2021) investigated the vibrational stability of motor casing made of Hemp fibre, Flax fibre, and their hybrid using FEA, finding that the hybrid material demonstrated higher stiffness and strength. Karandikar et al. [36] (2017) performed static structural analysis of crankshaft and camshaft materials for TATA Vista Quadrajet, comparing experimental and analytical stresses. Kumar et al. [37] (2020) studied heat transfer rate improvements in cooling fins with varied geometries using ANSYS. Giurgiu et al. [38] (2013) modeled static and dynamic behavior of radial tires for civil and military vehicles using FEA. Gautam et al. [39] (2013) performed static stress analysis of connecting rods made of SS 304 for Cummins engines using ANSYS. Yin et al. [40] (2018) optimized cutting blade design for double-sided offset paper heaps using ANSYS. Thriven et al. [41] (2013) conducted static analysis on a crankshaft of a single-cylinder I.C. engine, validating theoretical results with FEA. Lastly, Li et al. [42] (2011) used ANSYS for thermal and structural analysis of heat-exchange pipes, proposing methods for improved efficiency.

Thermal oil Paddler sludge dryer are effective as thermal oil has excellent thermal properties including high heat capacity and thermal conductivity. It efficiently transfers heat to the sludge promoting rapid drying. The paddle system in the dryer ensures uniform heating and consistent drying. FEA analysis of the paddle sludge dryer will provide valuable insights into their structural, thermal and dynamic behavior. It helps optimizing the design, improve performance, and enhance durability.

3. Vibration Analysis by Experimentation on Paddle Sludge Dryer

In vibrational analysis, the governing equations define the dynamic behaviour of a vibrating system. The type of equations depends on the type of system and the analysis to be carried out. The equations are the basis of vibrational analysis and are applied to calculate the natural frequencies, mode shapes, and response characteristics of the system. By solving these equations, engineers are able to comprehend and optimize the dynamic behavior of structures and machinery, making them reliable and effective.

The Equation of Motion is used to describe the dynamic behaviour of the system and is generally expressed as:

$$M \frac{d^2x}{dt^2} + C \frac{dx}{dt} + Kx = F(t) \quad (1)$$

Where M is the mass matrix, x is the displacement vector, t is time, C is the damping factor, K is the stiffness matrix, and $F(t)$ is the vector of applied external forces.

This equation considers the mass, damping, and stiffness characteristics of a multi-degree-of-freedom system. The natural frequency of a vibrating system is the frequency at which the system vibrates freely without any external excitation and can be calculated by solving the eigenvalue problem.

For experimental vibrational analysis of a SS 316 material paddle sludge dryer, certain properties are taken into account such as a modulus of elasticity of 193,000 N/mm², Poisson's ratio of 0.30, density of 7,850 Kg/m³, yield strength of 290 N/mm², and ultimate tensile strength of 580 N/mm². To detect the peak frequency of the paddle sludge dryer with an FFT (Fast Fourier Transform) analyser, the following steps are carried out. Initially, data collection is performed through vibration data gathering while the paddle sludge dryer operates with the help of an accelerometer placed at strategic points around Model-2, Model-3, and Model-4 of the assembly. The acquired data in time-domain signal format is transformed into a digital time-domain signal.

Subsequently, the FFT algorithm is applied to the pre-processed time-domain signal to transform it into the frequency domain. Once the frequency spectrum is obtained, it is analyzed to identify the peak frequency. The FFT analyser provides valuable insights into the vibration characteristics of the paddle sludge dryer, and the natural frequencies of the system can be determined by observing the FFT plot, where the peak values correspond to the natural frequencies. Case studies are carried out at areas of concern, and the experimental data obtained for all three models are analysed and explained to understand the vibrational behaviour of the system.

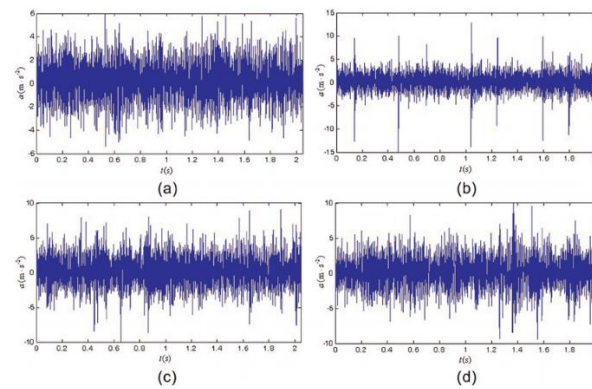


Fig 6: Experimental vibration results for Model 1, Model 2, Model 3 and Model-4

Hence from the experimental data obtained the Frequency obtained at the 1st mode shape of all the case is considered and latter it will be validated with the frequency obtained from the numerical analysis of the models.

Table 2: Frequency by experimentation

Mode Shape	Frequency, Hz
Case-1	13.53
Case-2	10.31
Case-3	5.80

This data received from the experimental method of vibration analysis will be compared to the numerical data to whether the data obtained is in the good correlation.

4. Finite Element Analysis of Paddler Sludge Dryer

Paddle Sludge Dryer model imported and converted to mesh model after splitting it into four subassemblies inline to achieve accurate numerical as well as analytical results. Finite element analysis on paddle sludge dryer is performed using ANSYS19R3 software. Paddle Sludge dryer is analysed using SHELL 281 and SOLID 186 elements. Four motors are used in the assembly of paddler sludge dryer. Actual motor geometries are not considered in FE Analysis but motors are modelled as point masses.

Further the CAD model is imported in ANSYS and the model is divided into finite elements to create a mesh. The SHELL 281 elements are meshed using quadrilateral and triangular elements. The choice between quadrilateral and triangular elements depends on the specific requirements. In this project combination of quadrilateral and triangular elements is used to provide more flexibility and accuracy in capturing the complex geometry and behaviour of the paddle sludge dryer. The Solid 186 elements are typically meshed with hexahedral meshing. This type of element is particularly suitable for solid objects with regular and irregular geometries. Below are the meshed models of paddle sludge dryer.

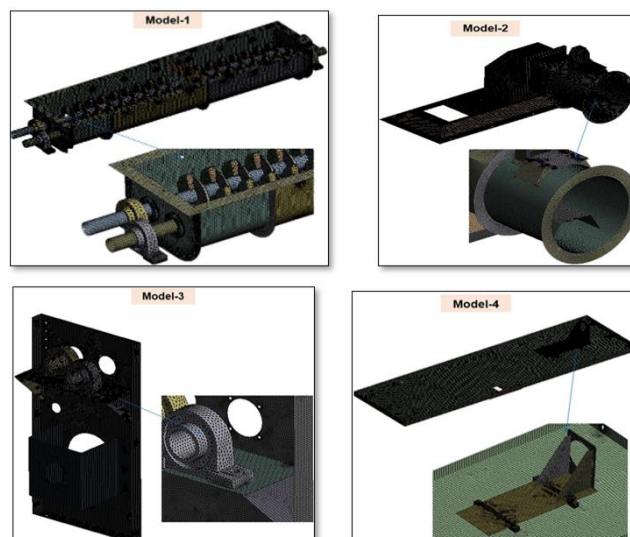


Fig 7: Meshing of models

4.1 Boundary Conditions:

Following type of load and boundary conditions are applied on each model respectively: -

A. Load and Boundary conditions for Model-1

In the FE model, gears and their arrangement, as well as the funnel and exhaust arrangements, are modeled using point masses. All bolted connections are defined using bonded contacts to ensure a rigid connection. A pressure equivalent to 500 kg of sludge is applied to the inner surface, along with additional pressure resulting from the friction of sludge against the blades. An acceleration due to gravity of 1G

(9.81 m/s²) is also applied throughout the model. Internal pressure of thermic oil at 2 bar is applied on all inner surfaces that come into contact with the thermic oil. Additionally, a thermal load of 230°C is applied from the inner surface of the jacket wherever it comes in contact with thermic oil, while a temperature of 50°C is applied to other parts of the assembly.

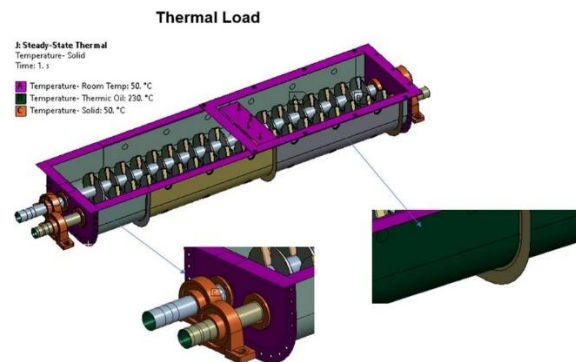


Fig 8: Thermal Load For Model-1

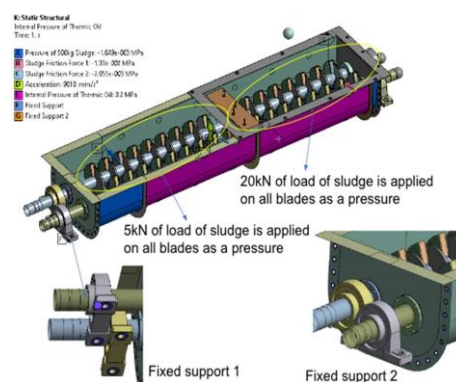


Fig 9: Load and Boundary Condition of Model-1

B. Load and Boundary Conditions for Model-2

The model is analyzed for both modal and structural analysis. Structural analysis is conducted to evaluate the model considering its self-weight, which is represented by the acceleration due to gravity of 1G (9.81 m/s²). Fixed supports are applied to the bolt hole locations to restrict movement, and all bolted connections are defined using bonded contacts to simulate rigid joints. In this FE model, the motor, exhaust fan, and funnel are represented using point masses with weight details of 10 kg for the motor, 5 kg for the exhaust fan, and 65 kg for the funnel. The Fig below illustrates the applied loads and boundary conditions applied to Model-2.

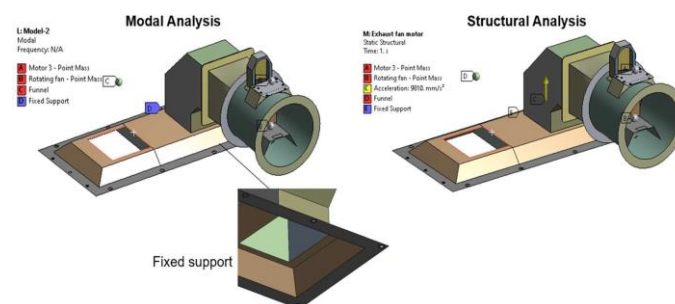


Fig 10: Load and Boundary Conditions for Model-2

C. Load and Boundary Conditions for Model-3

The model is analyzed for both modal and structural analysis. Structural analysis is carried out to evaluate the model under self-weight, which corresponds to an acceleration due to gravity of 1G (9.81 m/s²). Fixed supports are applied to the bolt hole locations as illustrated below. In this FE model, the motor and gear assembly, along with the weights of the shafts and blades acting on the bearings, are represented using point masses with weights of 91 kg, 67.5 kg, and 66.6 kg, respectively. Additionally, all bolted connections are defined using bonded contacts to ensure rigid connections throughout the model.

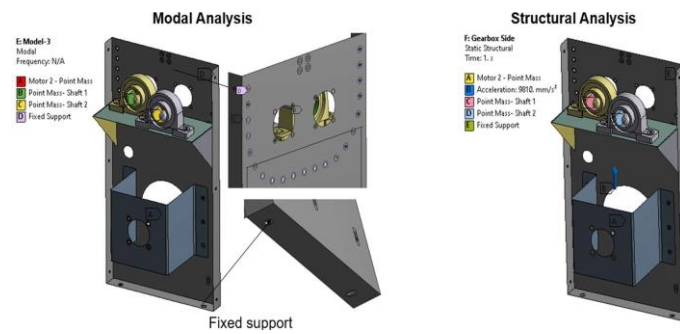


Fig 11: Load and Boundary Conditions for Model-3

D. Load and Boundary Conditions for Model-4:

In this FE model, the motor, oil, and tank are represented using point masses. All bolted connections are defined using bonded contacts to ensure rigid connections throughout the model. The model is analyzed for both modal and structural analysis. Structural analysis is performed to evaluate the model under self-weight, which corresponds to an acceleration due to gravity of 1G (9.81 m/s²). Fixed supports are applied to six bolt hole locations as illustrated below, providing necessary constraints to the model.

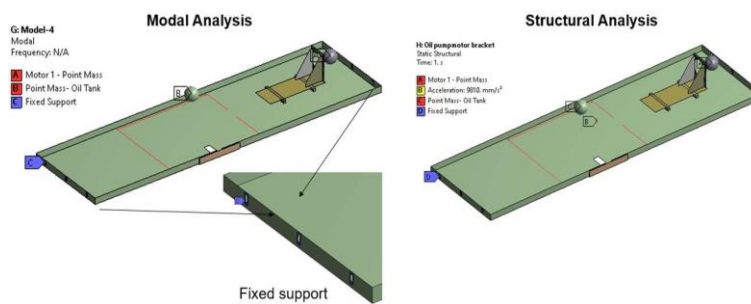


Fig 12: Load and Boundary Conditions for Model-4

4.2 Analysis based on the loads acting on the models

A. Thermal and structural analysis

As discussed above, Thermal and structural load act on the Model-1 of the paddler sludge dryer assembly. In this FE model, gears & its arrangement and funnel & exhaust arrangements are modelled using point masses.

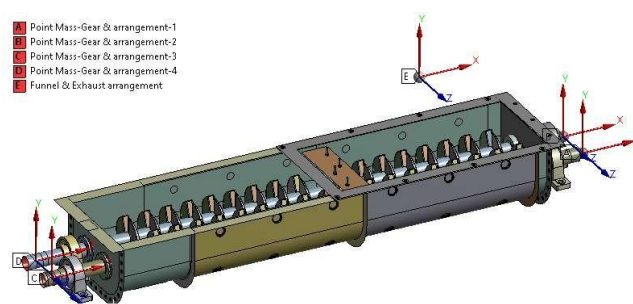


Fig 13: Point Masses on Model-1

The steady state thermal and static structural analysis are carried out the model-1 of paddle sludge dryer and the results obtained are as shown below.

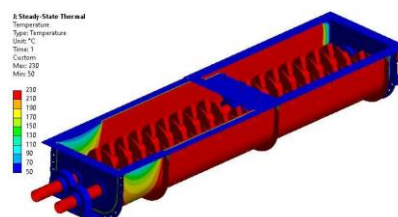


Fig 14: Steady state thermal analysis

The below given Fig shows the deformation plots for thermal + structural analysis of Model-1

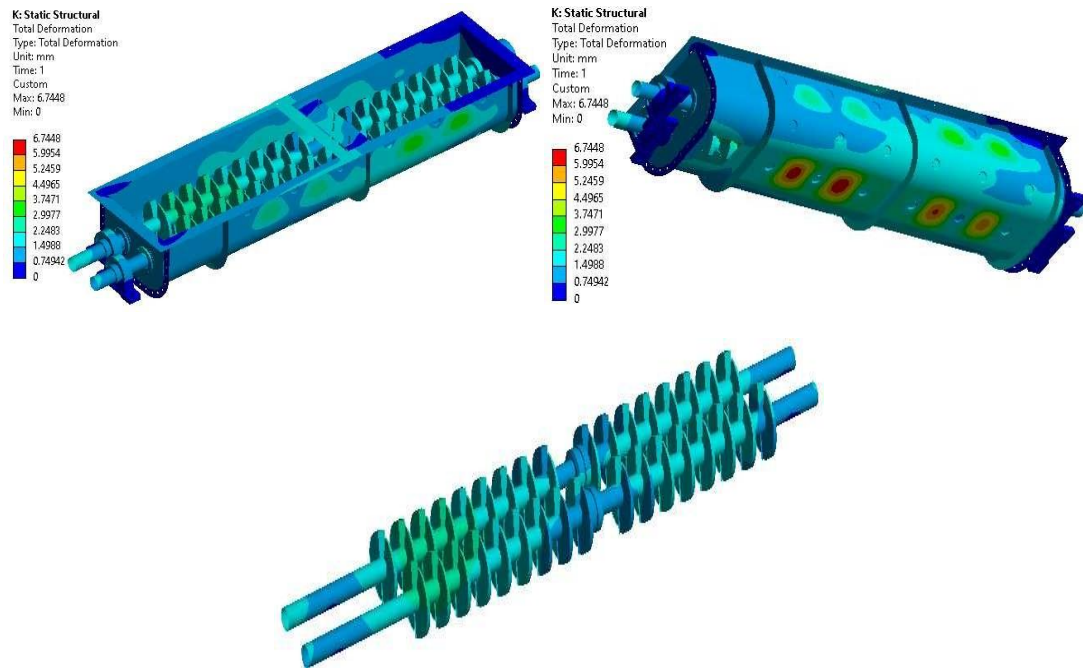


Fig 15: Deformation Plots for Thermal + Structural Analysis

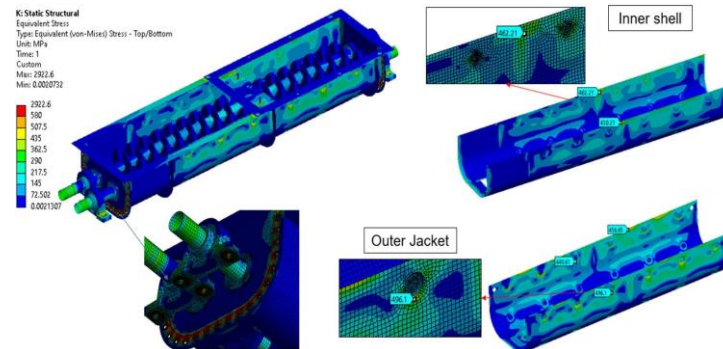


Fig 16: Stress Plots for Model-1

Hence from the result shown above we can see that overall equivalent stress of 496MPa is less than the Ultimate Tensile strength of 580MPa and all the Max. Equivalent stress are at the fixed supports and can be ignored as they are unrealistic. Thus we can say that the Model-1 of paddler sludge dryer assembly is safe to operate under given loading conditions.

B. Structural and Modal Analysis of Model-2

The Point masses acting on the system are as shown below:

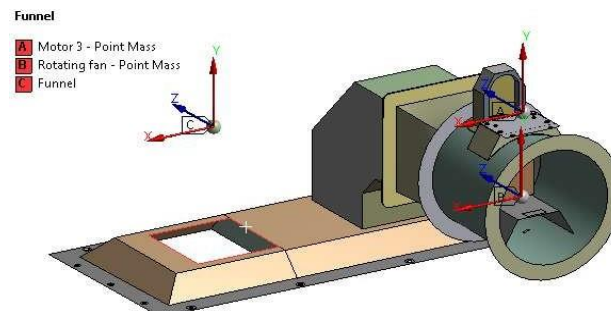


Fig 17: Point masses acting on Model-2

Below given are the solution of modal analysis with the different shade shape and frequencies shown in the table. Hence the solution obtained for 1st two mode shapes is as shown below

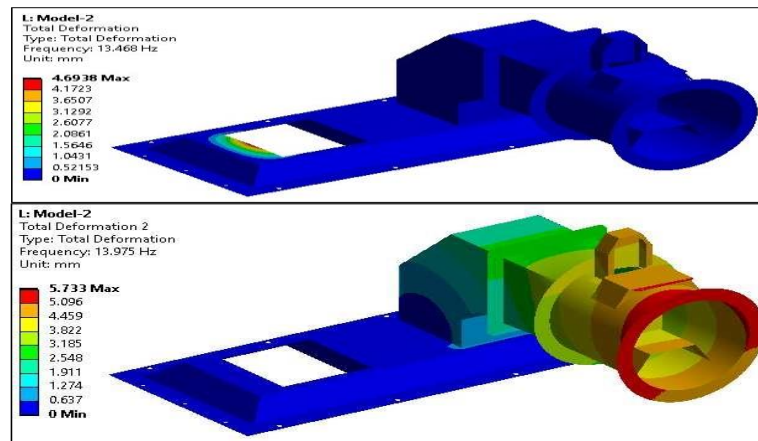


Fig 18: Modal Analysis Mode-1 and Mode-2

Below given table gives us the equivalent stress for model-2 of exhaust fan assembly

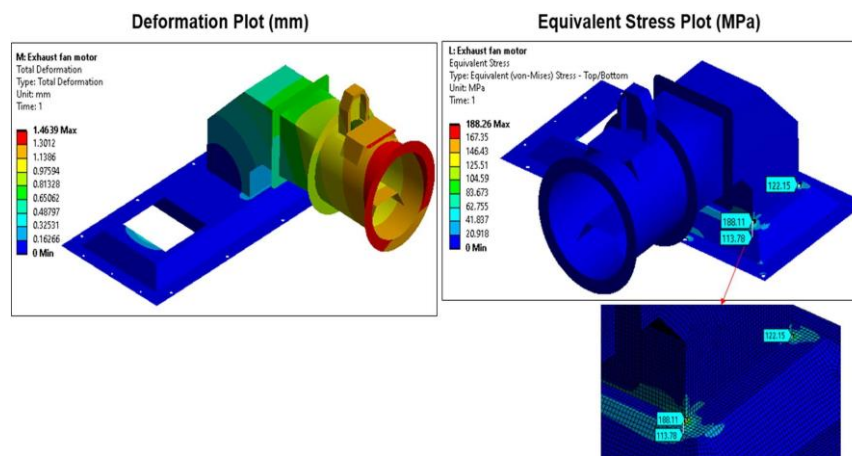


Fig 19: Structural Analysis for Model-2

Hence from the solution obtained it's observed that the mode of motor mounting bracket is at 13.9Hz. Motor running speed is 150-200 RPM i.e 2.5 to 3.3 Hz. The natural frequency of motor mounting bracket is far away from the excitation frequency of the motor and so, under motor operating conditions resonance will not occur.

Since, overall equivalent stress (188MPa) < Yield Strength (290MP), Model 2 of assembly of paddle sludge dryer is safe under given operating conditions.

C. Structural and Modal Analysis of Model-3

The point masses acting on the Model-3 are shown in the Fig below.

The below given Fig can be referred for the identification of the point masses on the model.

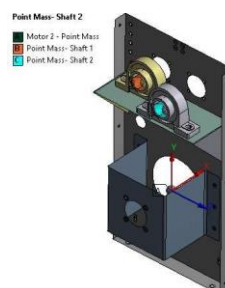


Fig 20: Point Masses Acting on Model-3

The solution received for the applied load and boundary condition is as discussed below:

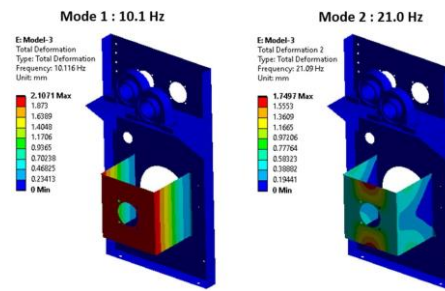


Fig 21: Modal Analysis for Mode shape 1&2

The result for structural analysis is as discussed below:

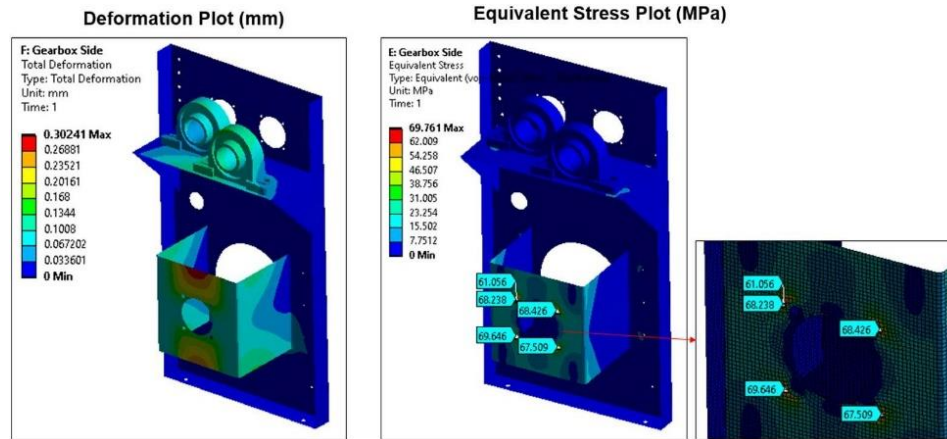


Fig 22: Structural Analysis of Model-3

The mode of the gear mounting bracket is identified at 10.1 Hz. The motor operates at a running speed of 150–200 RPM, which corresponds to a frequency range of 2.5 to 3.3 Hz. The natural frequency of vibration of the motor mounting bracket is 10.5 Hz, which is significantly higher than the excitation frequency of the motor (2.5–3.3 Hz). Therefore, resonance is not expected to occur under normal motor operating conditions. Additionally, the overall equivalent stress of 69 MPa is well below the yield strength of 290 MPa, indicating that Model-3 of the sludge dryer assembly is safe to operate under the specified loading conditions.

D. Structural and Modal Analysis of Model-4

In this FE model, motor and oil & tank are modelled using point masses.

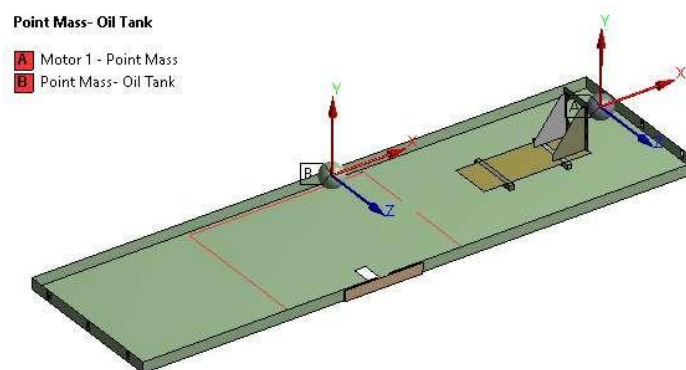


Fig 23: Point Mass acting on Model-4

Below are the results obtained for the Modal and structural analysis of Model-4:

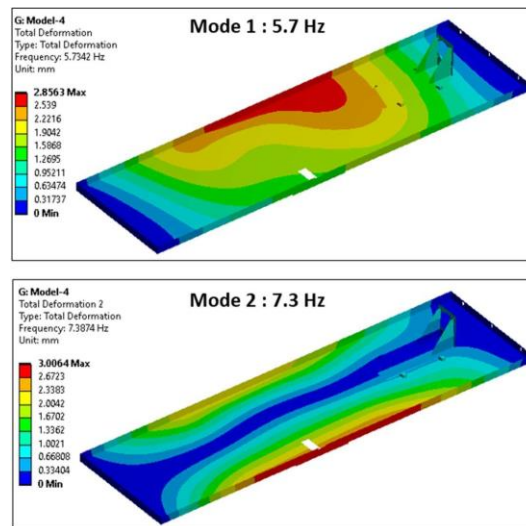


Fig 24: Modal Analysis for Model-4

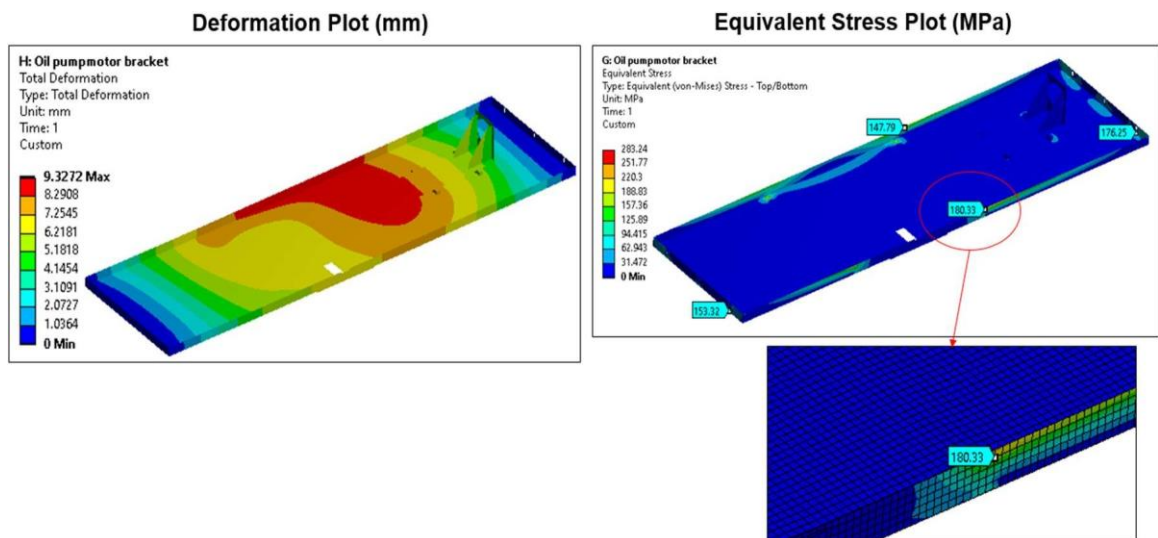


Fig 25: Structural Analysis for Model-4

Based on the results obtained, the mode of the motor mounting bracket is identified at 5.7 Hz. The motor operates at a running speed of 150–200 RPM, which corresponds to a frequency range of 2.5 to 3.3 Hz. The natural frequency of vibration of the motor mounting bracket (5.7 Hz) is significantly higher than the excitation frequency of the motor (2.5 to 3.3 Hz). Therefore, resonance will not occur under normal motor operating conditions. Additionally, the overall equivalent stress of 180 MPa is below the yield strength of 290 MPa, indicating that Model-4 of the assembly is safe to operate under the specified loading conditions.

5. Results and Discussion

The results from the various analyses conducted on Models 1, 2, 3, and 4 of the paddle sludge dryer assembly confirm the structural integrity and operational safety of the designs under specified conditions.

The results from the modal analysis in ANSYS, as presented in Table 2, indicate that Model 2 exhibits the highest natural frequencies across all mode shapes, followed by Model 3 and Model 4. For the first mode shape, Model 2 has a frequency of 13.4 Hz, whereas Model 3 and Model 4 show significantly lower frequencies at 10.1 Hz and 5.7 Hz, respectively. As the mode number increases, the frequency values also increase, with Model 2 maintaining the highest values, peaking at 97.3 Hz in the sixth mode. Model 3 follows a similar trend, with its highest frequency recorded at 89.5 Hz, whereas Model 4 shows the lowest overall frequencies, reaching a maximum of only 31.1 Hz in the sixth mode. These findings suggest that Model 2 exhibits greater structural stiffness compared to the other models.

Table 3 presents the equivalent stress values for all four models, demonstrating that Model 1 experiences the highest stress concentrations, with values ranging from 430.21 MPa to a peak of 496.1 MPa. In contrast, Model 2 shows significantly lower stresses, with a maximum of 188.11 MPa. Model 3 has even lower stress values, maintaining a range between 61.056 MPa and 69.646 MPa. Model 4 experiences intermediate stress levels, ranging from 147.79 MPa to 180.33 MPa. The absence of stress values for certain modes in Models 2 and 4 suggests potential limitations in stress distribution calculations. Overall, Model 1 exhibits the highest stress levels, indicating that it may be the least favorable design in terms of structural integrity, while Model 3 appears to have the most uniform stress distribution with relatively lower values.

Table 2: Frequencies for all models using Modal Analysis in ANSYS

Mode Shape	Frequency (Hz) for Model 2	Frequency (Hz) for Model 3	Frequency (Hz) for Model 4
1	13.4	10.1	5.7
2	13.9	21.0	7.3
3	20.5	31.4	11.1
4	21.5	50.0	19.9
5	82.6	85.4	26.1
6	97.3	89.5	31.1

Table 3: Equivalent Stresses for all four models

Sr. No.	Equivalent stress (MPa) for Model 1	Equivalent Stress (MPa) for Model 2	Equivalent Stress (MPa) for Model 3	Equivalent Stress (MPa) for Model 4
1	430.21	113.78	61.056	147.79
2	448.61	122.15	67.509	153.32
3	456.65	188.11	68.0238	176.25
4	462.61	-	68.426	180.33
5	496.1	-	69.646	-

The thermal and structural analysis of Model 1 indicates that the maximum equivalent stresses are concentrated at contact regions or fixed supports and are therefore ignored. The overall equivalent stress recorded for Model 1 is 496 MPa, which is lower than its ultimate strength of 580 MPa. This confirms that Model 1 remains structurally safe under the given operating conditions.

The modal analysis of Models 2, 3, and 4, performed using both experimental and numerical Finite Element Analysis (FEA) methods, shows strong agreement between the calculated and experimentally obtained natural frequencies. As shown in Table 4, the percentage error between the FEA and experimental results remains minimal, ranging from -0.009 to -0.020, demonstrating the accuracy of the numerical model. Additionally, the modal analysis results from ANSYS, detailed in Table 3, show that Model 2 exhibits the highest natural frequencies across all mode shapes, followed by Model 3 and Model 4. This suggests that Model 2 has greater structural stiffness, while Model 4 has the lowest overall frequencies, reaching a maximum of only 31.1 Hz in the sixth mode.

Table 4: Comparison of FE and experimental natural frequency

Model	Numerical FEA frequency in Hz	Experimental frequency in Hz	Percentage Error
1	13.4	13.53	-0.009
2	10.1	10.31	-0.020
3	5.7	5.80	-0.017

The structural analysis of Model 2 shows an overall equivalent stress of 188 MPa, which is well below the yield strength of 290 MPa, confirming its safety under applied loads. Similarly, Model 3 exhibits an equivalent stress of 69 MPa, significantly lower than the yield strength, making it the most stress-efficient design. Model 4 records an equivalent stress of 180 MPa, which is also within the safety limit. Overall, the analysis confirms that all models of the paddle sludge dryer assembly are structurally sound and can safely operate under various loading conditions. Model 3, with the lowest stress values, appears to have the most uniform stress distribution, while Model 2 demonstrates the highest structural stiffness due to its higher natural frequencies.

6. Conclusion

From the results of the FE analysis, several conclusions can be drawn. First, the maximum equivalent stresses induced in the assemblies of Model-1, Model-2, Model-3, and Model-4 of the paddle sludge dryer are all within the allowable stress limits, indicating that the assembly is safe to operate under the given conditions. The motor runs at a speed of 150–200 RPM, corresponding to a frequency range of 2.5 to 3.3 Hz, while the natural frequencies of vibrations of all models at motor mountings are well above this range. Therefore, no resonance will occur during motor operation.

Additionally, the results obtained from the Finite Element Analysis confirm that the paddle sludge dryer assembly is safe to operate under the specified loading conditions without requiring design optimization. However, it is noted that the natural frequencies of Modes 3 and 4 are slightly closer to the excitation frequency. To mitigate vibrations in Models 3 and 4, increasing the thickness of the gear mounting bracket and motor mounting bracket is recommended.

The analysis highlights the effectiveness of state-of-the-art technology, with the robust and compact design of the paddle sludge handling machine proving essential for industrial applications. This approach is crucial for sustainable development. The live results obtained through FEA tools demonstrate that the machine offers a highly accurate, precise, and economical solution for sludge drying industries.

References

- [1] Bennamoun L, Arlabosse P, and Léonard A (2013) Review on fundamental aspects of application of drying process to wastewater sludge. *Drying Technology* 28.
- [2] Demir S (2015) Economic optimization of indirect sewage sludge heat dryer. In *ASME Power and Energy*.
- [3] Chen JL, Chen WD, and Wang F (2016) Comparative study on drying characteristics of sewage sludge in two kinds of indirect heat drying equipment. In *Advances in Engineering Research*.
- [4] Flori M and Vilceanu L (2020) Analysis of sludge drying process in vacuum filters. *Journal of Physics* 1426.
- [5] Deng W, Su Y, and Weichao (2013) Theoretical calculation of heat transfer coefficient when sludge drying in a Nara-type paddle dryer using different heat carriers. *Procedia Environmental Science* 18.
- [6] Sapmaz S, Kaya D, and Kılıçaslan İ (2016) Thermal and process analysis of paddle sludge dryer. In *IMSEC*.
- [7] Arlabosse P, Chavez S, and Lecomte D (2005) Drying of municipal sewage sludge: From a laboratory scale batch indirect dryer to the paddle sludge dryer. *Journal of Chemical Engineering*.
- [8] Wang B and Wang Z (2019) Feasibility analysis of drying sludge using flue gas. In *International Conference on Energy*.
- [9] Zhang K, Du J, Liu X, and Zhang H (2016) Molten salt flow and heat transfer in paddle heat exchanger. *IIETA*.
- [10] Nimbarte VR and Khamankar SD (2023) Design and failure analysis of piston. *IJRASET* 2.
- [11] Bhagat R and Jibhakate YM (2012) Thermal analysis and optimization of IC engine piston using finite element method. *IJMERE* 2.

- [12] Havale SA and Wankhade S (2018) Design and analysis of gudgeon pin to minimize stress concentration: A review. *IJRASET* 6.
- [13] Sau SK, Pulinat KG, Moss PN, Ranjeet P, and Prabhu SS (2016) Thermal analysis of disc brake using ANSYS software. *IJAERD*.
- [14] Kamalakara K and Prakash TS (2014) Design and optimization of oil pan using finite element method. *IJESRT*.
- [15] Zhang Z, Wu P, and Zhang HH (2014) Contact stress analysis of V-band clamp and piping system. *International Journal of Engineering and Innovative Technology* 4.
- [16] Rajappan R and Vivekanandhan M (2013) Static and modal analysis of chassis by using FEA. *The International Journal of Engineering* 2.
- [17] Pandya HR, Pandya JG, and Acharya GD (2018) Vibration analysis of pump shaft using FEA software. *Trends in Mechanical Engineering & Technology* 8.
- [18] R I and Mohanty SC (2012) Study on free vibrational analysis using rectangular plate. *Procedia Engineering* 38.
- [19] Pingulkar P and S B (2016) Free vibration analysis of laminated composite plates using finite element method. *Sage Journal, Polymers and Polymer Composites*.
- [20] Hariharan V and Srinivasan PSS (2009) Vibration analysis of misaligned ball bearings system. *International Journal of Science and Technology* 2.
- [21] Yamuna P and Sambasivarao K (2017) Modal analysis of beam with varying crack depth. *IRJET* 4.
- [22] Weis P (2017) Modal analysis of gearbox housing with applied load. *Procedia Engineering* 192.
- [23] Nigade RV, Bhide AM, and Jadhav TA (2014) Vibration analysis of gearbox casing component using FEA tool ANSYS and FFT analyser. *IJERT* 3.
- [24] Chaphalkar SP, Khetre SN, and Meshram AM (2015) Modal analysis of cantilever beam structure using finite element method and experimental analysis. *American Journal of Engineering Research* 4.
- [25] Darapureddy P, Srinivas C, and Narayana RL (2013) Static and modal analysis of base frame for steam turbine. *IJERT* 2.
- [26] Hebbal MS and Dabair M (2019) Static structural, modal and harmonic analysis for alloy car wheel rim using ANSYS workbench. *IJERT* 8.
- [27] Gukendran R, Sambathkumar M, and Sabari C (2022) Structural analysis of composite wind turbine using ANSYS. *Materials Today: Proceedings* 50.
- [28] Narendranath G and Suresh S (2012) Thermal analysis of gas turbine rotor blade by using ANSYS. *IJERA* 2.
- [29] Naser MQ, Kumar AVSS, and Gupta AS (2013) Structural and thermal analysis of a pressure vessel by using ANSYS. *International Journal of Scientific Engineering and Technology Research* 2.
- [30] Silori P, Shaikh A, Kumar KCN, and Tandon T (2015) Finite element analysis of traction gear using ANSYS. *Materials Today: Proceedings* 2.
- [31] Ooi J, Wang X, Tan C, Ho J, and Lim YP (2012) Modal and stress analysis of gear train design in portal axle using finite element modeling and simulation. *Journal of Mechanical Science and Technology*.
- [32] VBC L, RM, and IR (2012) Static analysis of an isotropic rectangular plate using finite element analysis. *Journal of Mechanical Engineering Research* 4.
- [33] Raghavendra M, Hussain SA, Pandurangadu V, and PalaniKumar K (2012) Modeling and analysis of laminated composite leaf spring under static load conditions by using FEA. *IJMERE* 2.
- [34] Vegi LK and Vegi VG (2013) Design and analysis of connecting rod using forged steel. In *Proceedings*.
- [35] Srinivasan T, Sharavanan S, NE, Sethuvelappan S, and RP (2022) Modal analysis of electrical motor casing. *IOP Conference Series: Materials Science and Engineering* 1112.
- [36] Karandikar KV, Deshpande SP, Patil SN, and Deshpande SA (2017) Design, modeling, FEM and experimental analysis of crankshaft and camshaft of a passenger car. *International Journal of Engineering Research in Mechanical and Civil Engineering* 2.
- [37] Kumar R and Singh D (2020) Static thermal analysis of fins models using ANSYS. *IJMET* 11.
- [38] Giurgiu T, Ciortan F, and Pupaza C (2013) Static and transient analysis of radial tires using ANSYS. In *Recent Advances in Industrial and Manufacturing Technologies*.
- [39] Gautam A and Ajit KP (2013) Static stress analysis of connecting rod using finite element approach. *IOSR Journal of Mechanical and Civil Engineering* 10.
- [40] Yin Z and Xu L (2018) Finite element analysis and optimization of paper cutter cutting blade on ANSYS. In *International Conference on Robots and Intelligent System*.
- [41] Thriveni K and JayaChandraiah B (2013) Modal analysis of a single cylinder 4-stroke engine crankshaft. *International Journal of Scientific and Research Publications* 3.
- [42] Li F, Xing J, and Liu Y (2011) Thermal analysis and stress analysis of heat exchange pipe based on ANSYS. In *Fourth International Conference on Information and Computing*.